Electronic Supplementary Material (ESI) for ChemComm.

Electronic Supplementary Information (ESI)

Functionalisation of MUF-15 Enhances CO_2/CH_4 Selectivity in Mixed-Matrix Membranes

Yiming Zhang [a], Elnaz Jangodaz [a],Ben Hang Yin * [b,c], and Shane G. Telfer * [a]

Table of Contents

1.Experimental section

Materials

Cobalt(II) acetate tetrahydrate (99.99%), isophthalic acid (H_2ipa, $C_8H_6O_4$, 99%), 5-fluoroisophthalic acid ($C_8H_5FO_4$, 98%), 5-bromoisophthalic acid ($C_8H_5BrO_4$, 98%), 5-nitroisophthalic acid ($C_8H_5NO_6$, 98%) and 5-methylisophthalic acid ($C_9H_8O_4$, 97%) were purchased from Sigma-Aldrich. Methanol (MeOH, 99.9%) was purchased from Fisher Chemicals. Polyimide of 6FDA-DAM (Mw ~ 326000, PDI ~ 2.68) was supplied by Akron Polymer Systems. Dichloromethane (DCM) was purchased from Sigma-Aldrich

Characterization

X-ray diffraction (XRD) patterns were recorded on a Bruker D8 Venture diffractometer with Cu_α radiation (wavelength = 1.54018 Å), with a diamond microfocus X-ray source and a Photon III 28 detector. Scanning Electron Microscope (SEM) images were taken on a FEI Quanta 200 Environmental with EDAX module. Thermogravimetric analysis (TGA) data were collected using the TA Q50 instrument at a heating rate of 10 °C/min from 50 to 600 °C with a N_2 flow rate of 40 mL/min. ATR-FTIR measurements used a Nicolet iS5 IR with iD7 ATR Accessory. Gas adsorption isotherms were measured on a Quantachrome Autosorb iQ2 instrument using ultra-high purity gases.

Synthesis of MUF-15 and its analogues

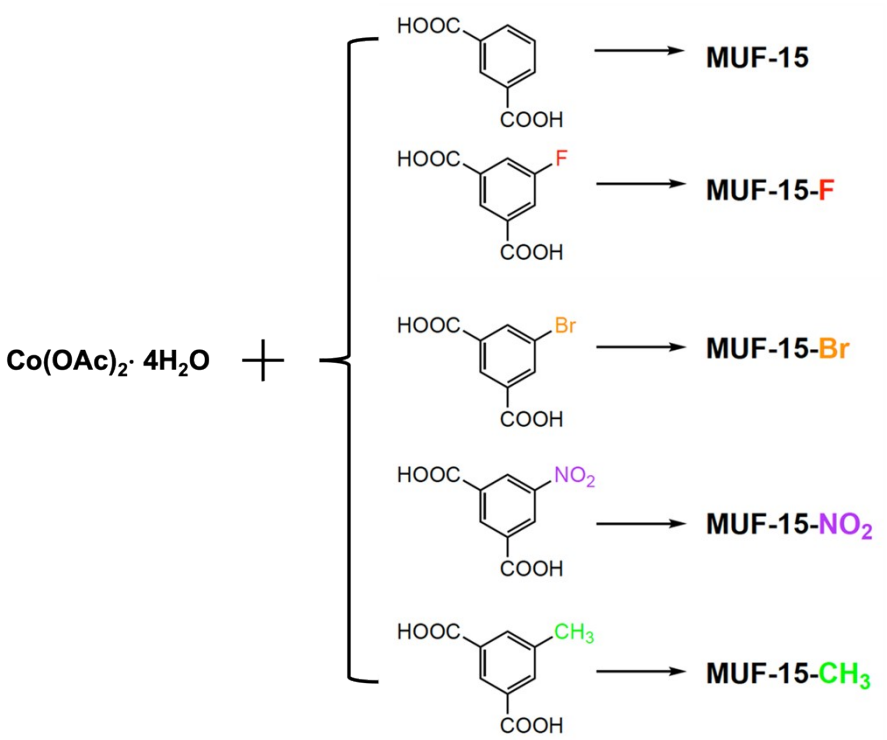

Figure S1. Scheme of the synthetic routes to MUF-15 and its analogues.

A mixture of $Co(OAc)_2{\cdot}4H_2O$ (125 mg, 0.5 mmol), organic ligands, MeOH (6 mL), and H_2O (0.5 mL) was sonicated for 10 min and sealed into a 25 mL Teflon-lined autoclave, then heated to the target temperature (Table S1). After cooling to room temperature, the resulting crystals were collected and washed with MeOH three times and then stored in MeOH for further use.

Table. S1 Synthesis conditions for MUF-15 and its analogues.

MOF	Metal	Ligand	L/M molar ratio	Reaction temp. (°C)	Reaction time (h)
MUF-15	$Co(OAc)_2{\cdot}4H_2O$	H_2ipa	2	120	48
MUF-15-F	$Co(OAc)_2{\cdot}4H_2O$	H_2ipa-F	1.75	120	24
MUF-15-Br	$Co(OAc)_2{\cdot}4H_2O$	H_2ipa-Br	2	120	48
MUF-15-NO_2	$Co(OAc)_2{\cdot}4H_2O$	H_2ipa-NO_2	1.75	120	48
MUF-15-CH_3	$Co(OAc)_2{\cdot}4H_2O$	H_2ipa-CH_3	1.75	140	36

Membrane fabrication

The MOF crystals (30 mg) were first dispersed in MeOH (10 mL) and then sonicated in an ultrasonic bath with a cooling water circulation system under 40 Hz for 1 h. The MOF powders were centrifuged to remove the solvent and washed with DCM three times. Subsequently, requisite masses of fillers were added into DCM (3 mL) and stirred overnight. Then 6FDA-DAM was added to solution, which was stirred for another 12 hours. The casting solution was then poured into a glass Petri dish on a level surface and left in a desiccator (30 cm in diameter) with DCM atmosphere at room temperature overnight. Finally, the resulting MMM was peeled off from the dish and treated in a vacuum oven at 130 ^{o}C for 2 hours to remove the residual solvent. The prepared membrane was immediately used for the gas permeability test.

Gas permeability measurement

Gas permeation tests were carried out with a Wicke-Kallenbach apparatus.[1] The membranes were fixed in a module sealed with an O-ring (Fig. S10). All tests were carried out at 20 ^{o}C with a feed pressure of 2 bar. The flow rate was controlled using Alicat mass flow controllers (MFC). Helium (20 SCCM) was used as the carrier gas in each test. The concentration of permeate gas was analyzed via a mass spectrometer (UGA-200, SRS). The total volume flow rate for the mixed-gas permeation tests was 20 SCCM with a CO_2/CH_4 molar ratio of 1:1. The gas permeability and selectivity were calculated using the Equations below:

$$P_i = \frac{Q_i \times L}{\Delta P_i \times A} \quad (1)$$

$$a_{i/j} = \frac{P_i}{P_j} \quad (2)$$

where P presents the gas permeability [1 Barrer = 10^{-10} cm^3 (STP)·cm/cm^2·s·cmHg], Q presents the volume flow rate of permeate gas [cm^3 (STP)/s], L presents the membrane thickness (cm), ΔP presents transmembrane pressure (cmHg) and A presents the membrane area (cm^2).

The CO_2 and CH_4 adsorption isotherms were fitted by Langmuir model as listed in equation below:

$$q = \frac{q_{sat,1} \times b_1 \times p}{1 + b_1 \times p} + \frac{q_{sat,2} \times b_2 \times p}{1 + b_2 \times p} \quad (3)$$

where q represents the gas concentration adsorbed, p represents the testing pressure, q_{sat} represents the saturation loadings for different sites, b_1 and b_2 represent the Langmuir parameters for different sites, if required.

The gas solubility (S) in the membrane was calculated using equation below:

$$S_i = \frac{q_i}{p_i} \quad (4)$$

The gas transportation through the membranes follows a solution-diffusion mechanism, therefore the gas diffusivity in the membranes is given by:

$$D_i = \frac{P_i}{S_i} \quad (5)$$

2.Supplementary Figures

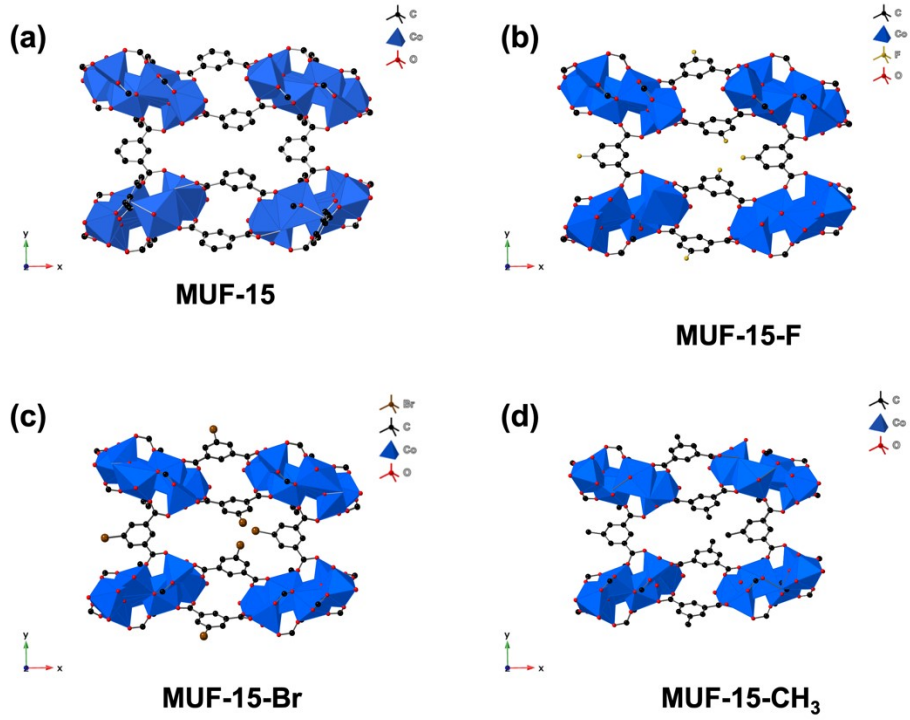

Figure S2. PXRD patterns of as-synthesized and calculated (a) MUF-15-Br and (b) MUF-15-CH_3.

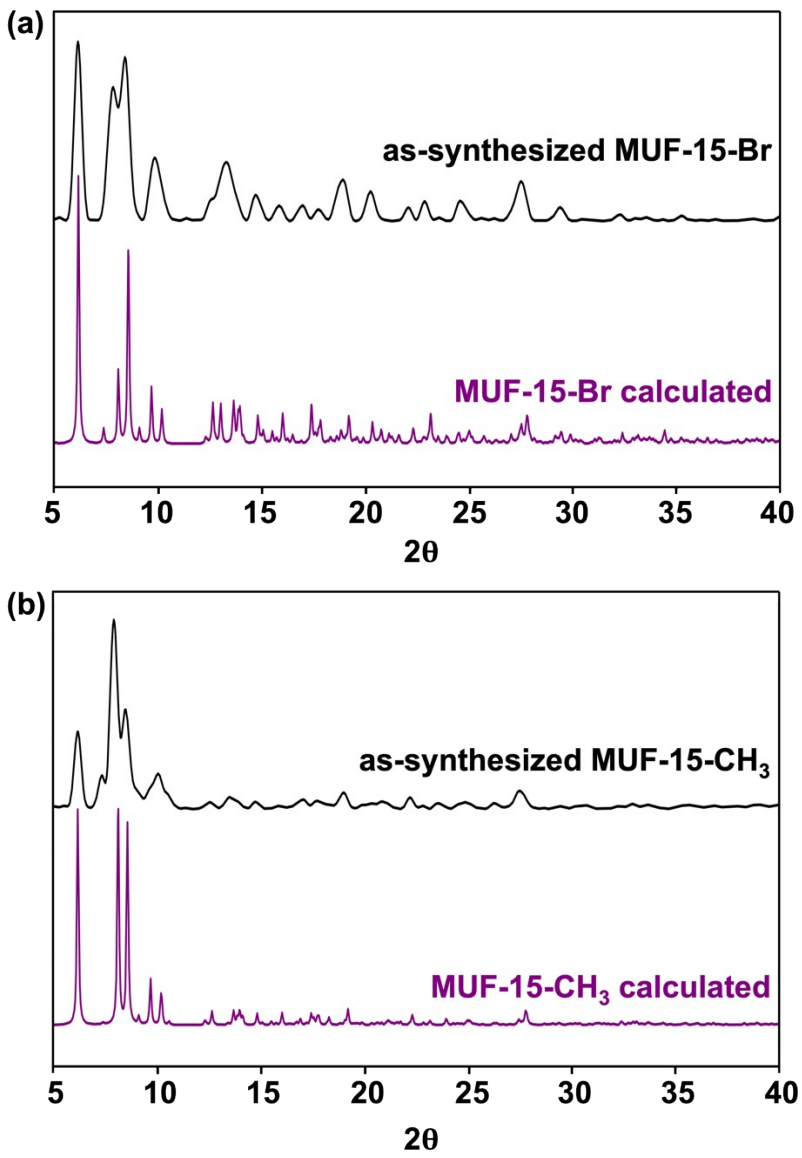

Figure S3. PXRD patterns of as-synthesized and calculated (a) MUF-15-Br and (b) MUF-15-CH_3.

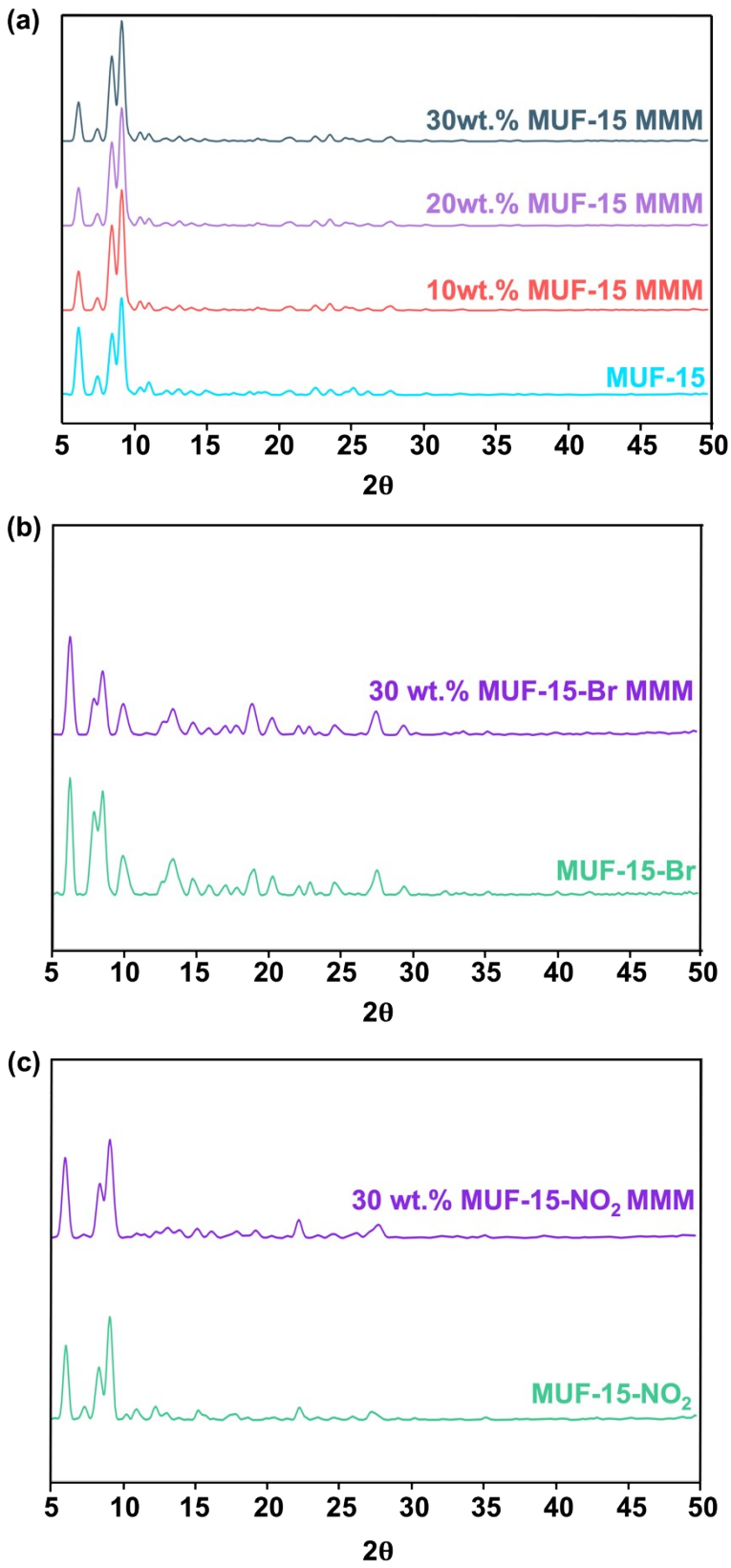

Figure S4. XRD patterns of MMMs with (a) MUF-15 (10 – 30 wt.%), (b) 30 wt.% MUF-15-Br, and (c) 30 wt.% MUF-15-CH_3.

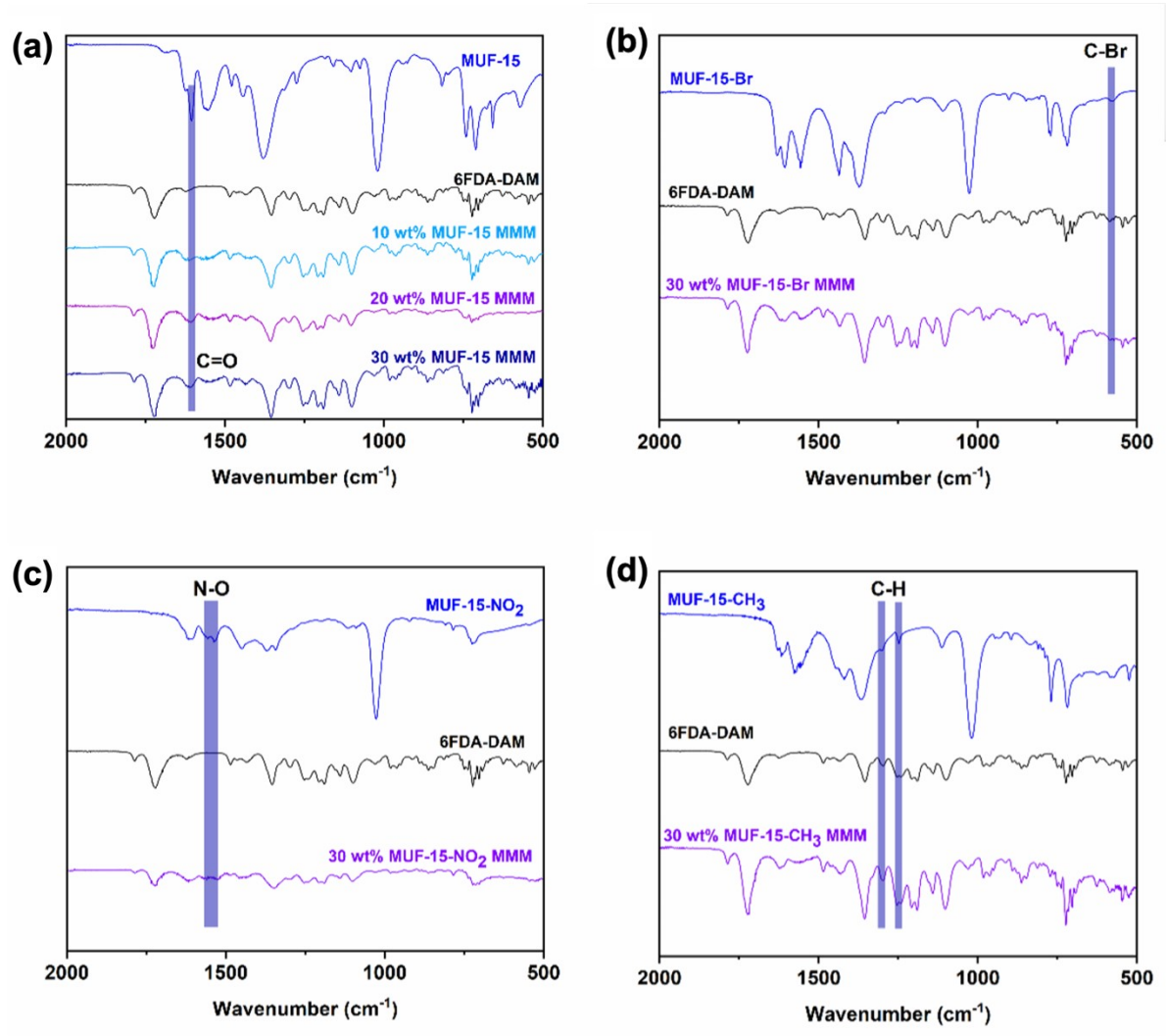

Figure S5. FTIR spectra of MMMs with (a) MUF-15, (b) MUF-15-Br, (c) MUF-15-NO_2, and (d) MUF-15-CH_3.

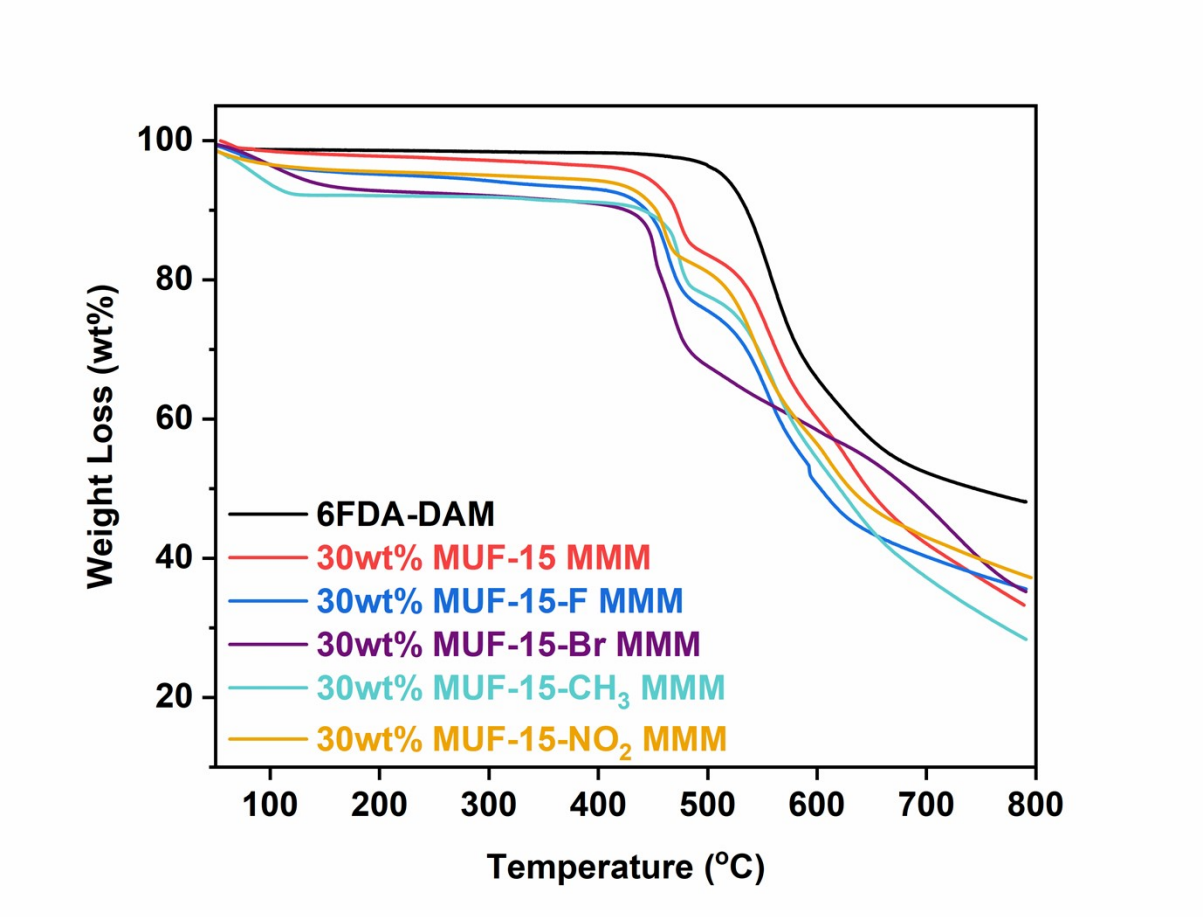

Figure S6. TGA curves of a pristine 6FDA-DAM membrane and MMMs incorporated with 30 wt.% MUF-15 and functionalized fillers.

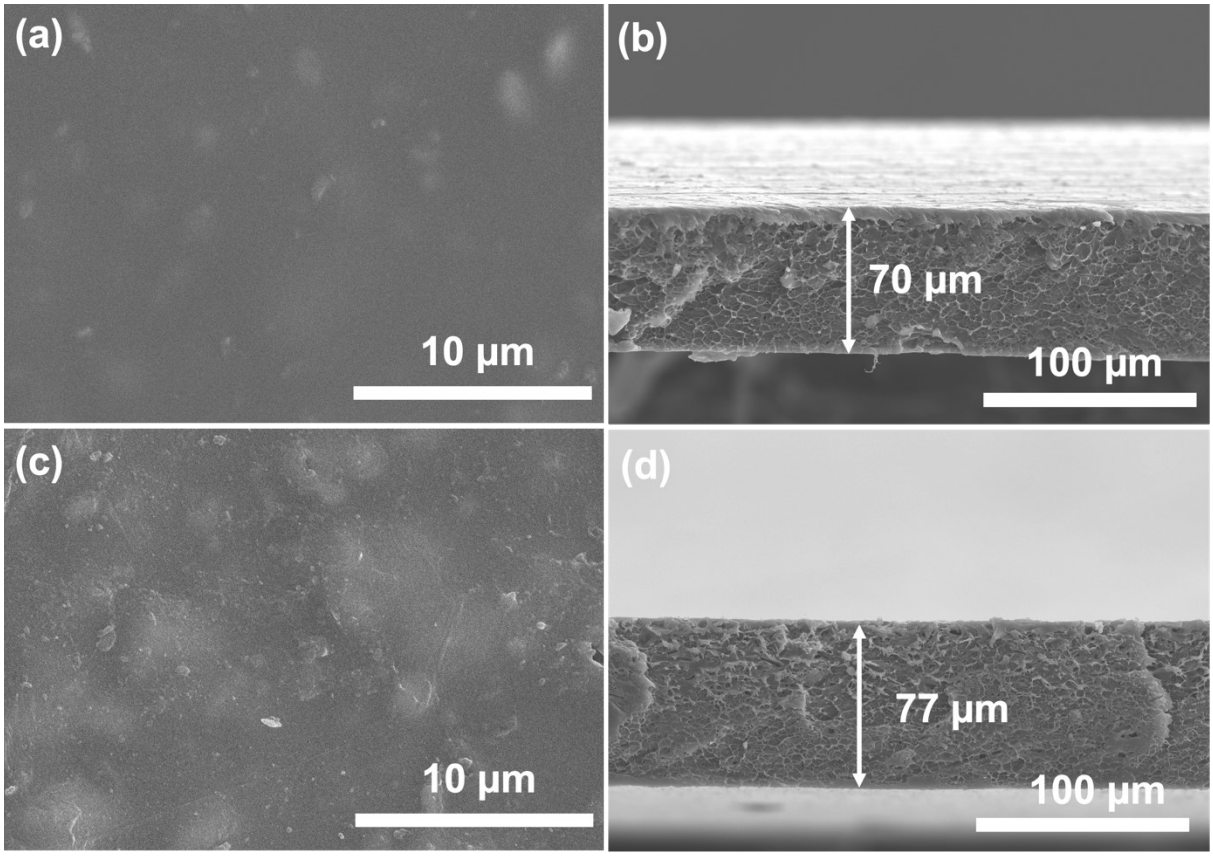

Figure S7. SEM images (a,b) 10 wt.% MUF-15 MMM and (c,d) 20 wt.%. MUF-15 MMM, Left: Surface. Right: Cross-section.

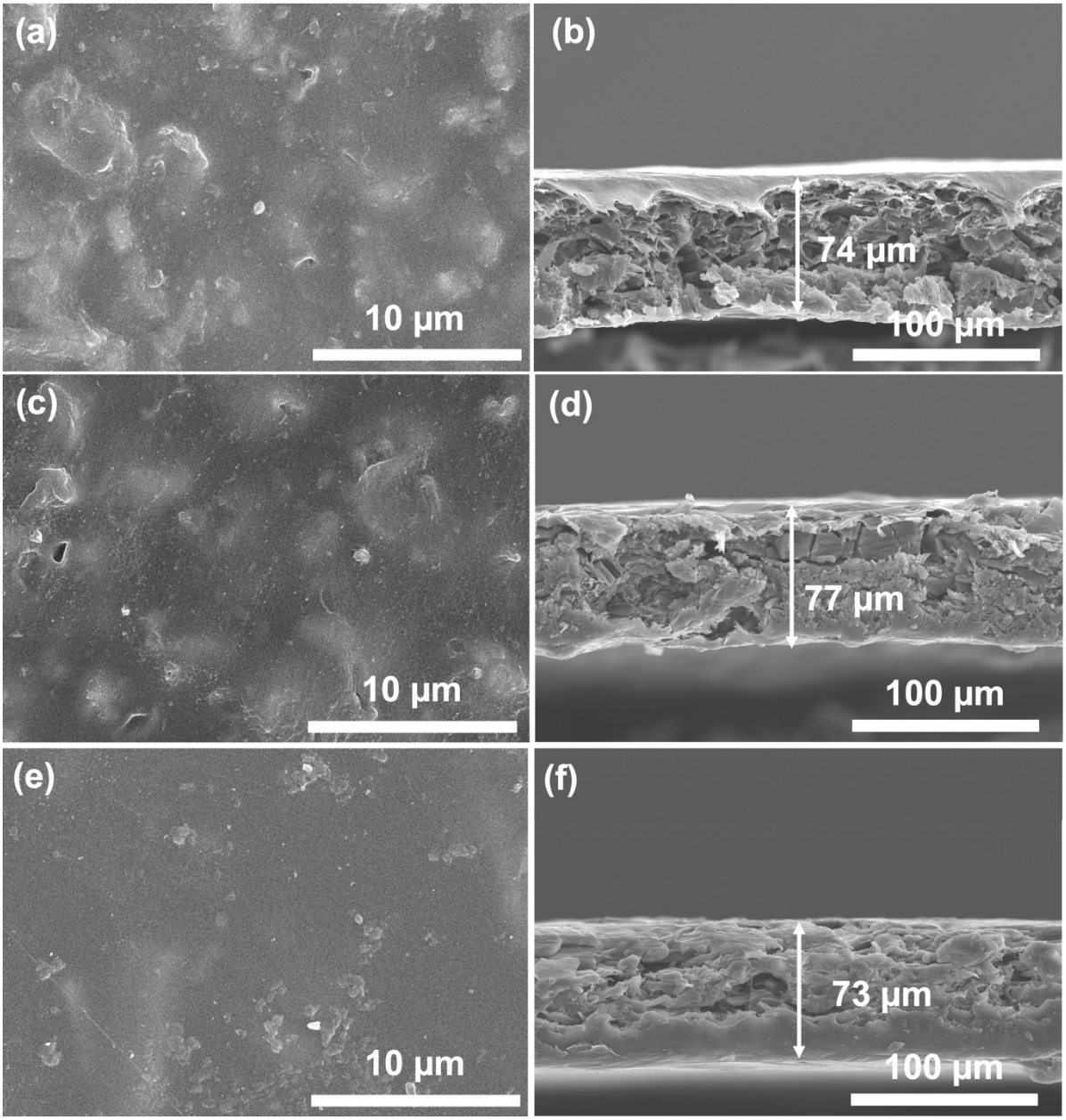

Figure S8. SEM images (a,b) 30 wt.% MUF-15-NO_2 MMM, (c,d) 30 wt.%. MUF-15-Br MMM and (e,f) 30 wt.% MUF-15-CH_3 MMM,

Left: Surface. Right: Cross-section.

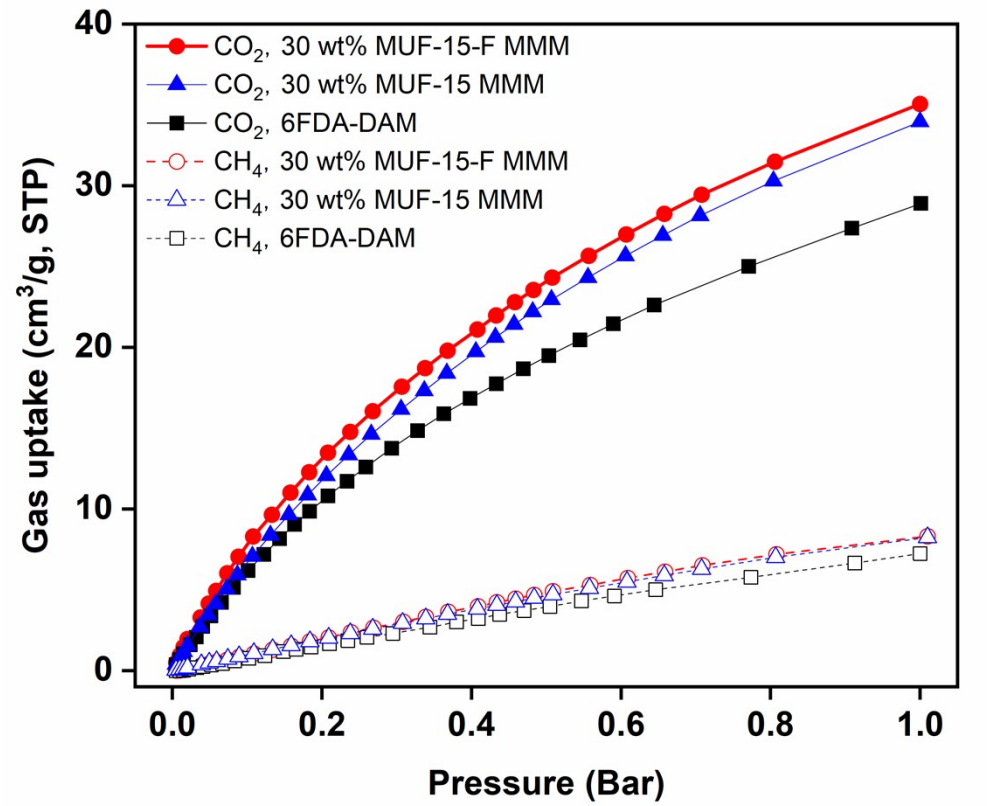

Figure S9. CO_2 and CH_4 adsorption isotherms at 293 K of a pristine 6FDA-DAM membrane and the MMMs incorporated with 30 wt.% MUF-15 and MUF-15-F.

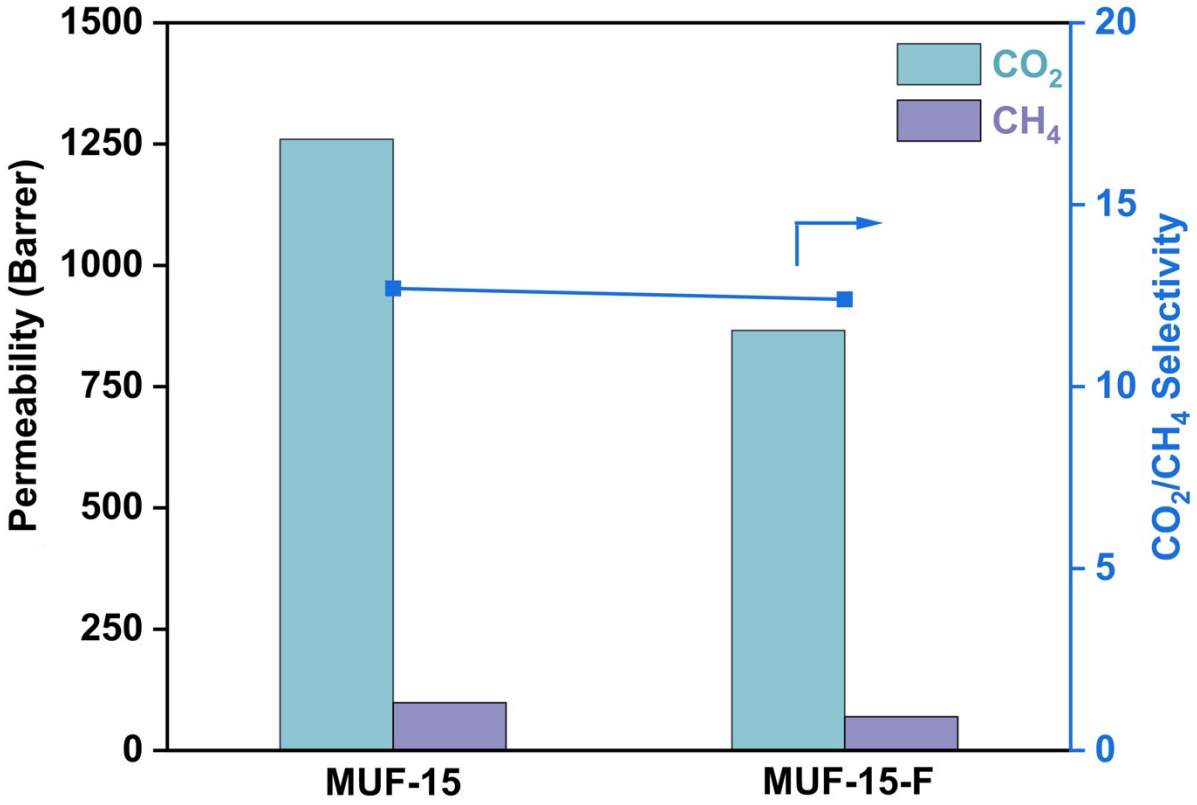

Figure S10. Binary gas permeation results for the MMMs incorporated with 30 wt.% MUF-15 and MUF-15-F.

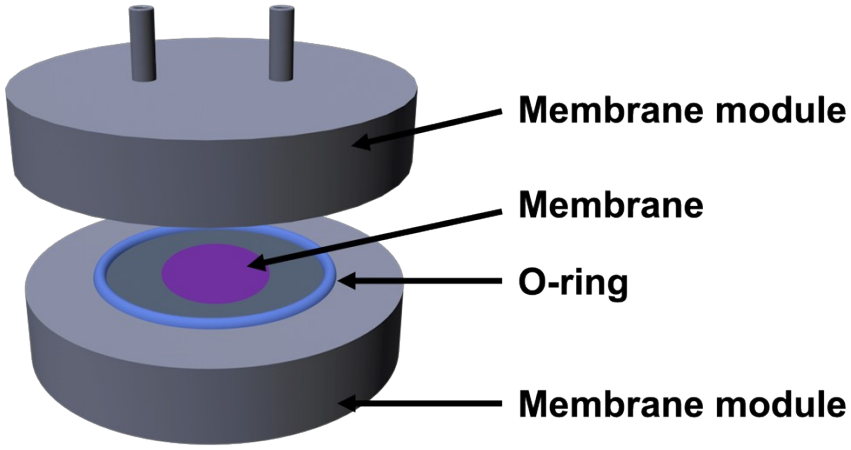

Figure S10. Schematic diagram of membrane sealed in the module with an O-ring.

Table S2 Fitting parameters for the adsorption isotherms.

Gas	Sample	Fitting Parameters				
		$q_{sat,1}$ (cm^3/g)	b_1 (Bar^{-1})	$q_{sat,2}$ (cm^3/g)	b_2 (Bar^{-1})	R^2
CO_2	6FDA-DAM	1840	0.0051	28.1	2.20	0.9999
	30 wt.% MUF-15 MMM	57.8	1.31	--	--	0.9997
	30 wt.% MUF-15-F MMM	66.6	0.70	9.13	5.90	0.9999
CH_4	6FDA-DAM	78.2	0.0392	121.6	0.039	0.9990
	30 wt.% MUF-15 MMM	35.7	0.21	12.2	0.21	0.9999
	30 wt.% MUF-15-F MMM	77.4	0.13	--	--	0.9987

Table S3 Pure (single) gas separation performance of the MMMs.

Membrane	Permeability (*Barrer*)		Selectivity
	CO_2	CH_4	CO_2/CH_4
6FDA-DAM	839	41.2	20.4
10 wt.% MUF-15 MMM	918	70.8	13.0
20 wt.% MUF-15 MMM	1220	79.9	15.3
30 wt.% MUF-15 MMM	1540	89.2	17.3
30 wt.% MUF-15-NO_2 MMM	1430	42.4	33.7
30 wt.% MUF-15-F MMM	1300	35.0	37.1
30 wt.% MUF-15-Br MMM	8090	1600	5.1
30 wt.% MUF-15-CH_3 MMM	11400	1440	7.9

Table S4 Gas solubilities and diffusivities in pristine 6FDA-DAM, 30 wt.% MUF-15 MMM and 30 wt.% MUF-15-F MMM.

	Solubility (10^3 mol/m^3·bar)		**Diffusivity** ($\times10^{-12}$ m^2/s)		CO_2/CH_4	
	CO_2	CH_4	CO_2	CH_4	Solubility selectivity	Diffusivity selectivity
6FDA-DAM	4.24	0.46	6.63	2.97	9.13	2.23
30 wt.% MUF-15 MMM	4.39	0.59	11.73	5.05	7.43	2.33
30 wt.% MUF-15-F MMM	6.07	0.61	7.18	1.94	10.02	3.71

Table S5 Gas separation performance of selected polyimide MMMs from the literature.

Filler	Filler content (wt. %)	Testing Conditions		CO_2 Permeability (Barrer)	CO_2/N_2 Selectivity	Ref
		P (bar)	T (˚C)			
MIL-53	25	10.3	35	20.8	44	[2]
MIL-53-NH_2	30	10.3	35	14.6	79.8	[2]
LaBTB	10	3.5	20	725	35	[3]
MOF-199	24	3	35	28	89	[4]
MIL-101(Cr)	24	4	25	50	50	[4]
Y-fum-fcu-MOF	30.05	6.9	35	587.9	29.3	[5]
Ni_2(dobdc)	25	--	--	715	14.5	[6]
KAUST-7-NH_2	50	2	35	568.5	36.2	[7]
UiO-66	14	2	35	1912	30.8	[8]
UiO-66-NH_2	16	2	35	1223	29.8	[8]
ZIF-8	10	4.8	30	687.2	8.92	[9]
ZIF-90	15	2	25	720	36.9	[10]
SSZ-16	5	2	25-35	365	34.8	[11]
HKUST-1	20	3.5	35	1560	18.8	[12]
MUF-15	30	2	20	1540	17.3	This work
MUF-15-NO_2	30	2	20	1430	33.7	This work
MUF-15-F	30	2		1300	37.1	This work

3.References

1. H. Yin, A. Alkas, Y. Zhang, Y. Zhang and S. G. Telfer, *J. Membr. Sci.*, 2020, 118245.
2. X. Y. Chen, H. Vinh-Thang, D. Rodrigue and S. Kaliaguine, *Ind. Eng. Chem. Res.*, 2012, **51**, 6895-6906.
3. Y. Hua, H. Wang, Q. Li, G. Chen, G. Liu, J. Duan and W. Jin, *J. Mater. Chem. A.*, 2018, **6**, 599-606.
4. A. Nuhnen, M. Klopotowski, H. B. Tanh Jeazet, S. Sorribas, B. Zornoza, C. Téllez, J. Coronas and C. Janiak, *Dalton Trans.*, 2020, **49**, 1822-1829.
5. G. Liu, V. Chernikova, Y. Liu, K. Zhang, Y. Belmabkhout, O. Shekhah, C. Zhang, S. Yi, M. Eddaoudi and W. J. Koros, *Nat. Mater.*, 2018, **17**, 283-289.
6. J. E. Bachman and J. R. Long, *Energy Environ. Sci.*, 2016, **9**, 2031-2036.
7. L. Wang, X. Bai, Y. Gu, X. Shi, S. Wang, J. Hua, R. Hou, C. Wang and Y. Pan, *Adv. Mater. Interfaces.*, 2023, **10**, 2202524.
8. M. Z. Ahmad, M. Navarro, M. Lhotka, B. Zornoza, C. Téllez, W. M. de Vos, N. E. Benes, N. M. Konnertz, T. Visser, R. Semino, G. Maurin, V. Fila and J. Coronas, *J. Membr. Sci.*, 2018, **558**, 64-77.
9. N. Jusoh, Y. F. Yeong, K. K. Lau and A. M. Shariff, *J. Clean. Prod.*, 2017, **149**, 80-95.
10. T.-H. Bae, J. S. Lee, W. Qiu, W. J. Koros, C. W. Jones and S. Nair, *Angew. Chem. Int. Ed.*, 2010, **49**, 9863-9866.
11. M. Z. Ahmad, V. Martin-Gil, T. Supinkova, P. Lambert, R. Castro-Muñoz, P. Hrabanek, M. Kocirik and V. Fila, *Sep. Purif. Technol.*, 2021, **254**, 117582.
12. C. Duan, X. Jie, H. Zhu, D. Liu, W. Peng and Y. Cao, *J. Appl. Polym. Sci.*, 2018, **135**, 45728.